coatings

Article

Hydration Heat and Hydration Kinetics of Cement Paste Compound with Molybdenum Tailings Powder: A Research Article

Qinghui Cheng [1], Weiqi Meng [2,*] and Kunlin Ma [2,*]

[1] School of Intelligent construction, Fuzhou University of International Studies and Trade, Fuzhou 350202, China; qinhui.cheng@qdc.edu.cn
[2] School of Civil Engineering, Central South University, Changsha 410075, China
* Correspondence: 214812296@csu.edu.cn (W.M.); makunlin@csu.edu.cn (K.M.)

Abstract: Molybdenum tailings powder (MTs) has potential pozzolanic activity and can be used as a mineral admixture. In order to comprehend the influence of MTs powder on the cement hydration process, the hydration heat and kinetics of composite cementitious materials (CCMs) were investigated using an isothermal calorimeter and the Krstulovic–Dabic model. Furthermore, the influences of fly ash (FA), slag (SL), and MTs powder on hydration heat were compared and analyzed, considering the same content. The results show that the proper amount of MTs can promote the hydration of CCMs. When the content of MTs is 5% and 15%, the second exothermic peak of the CCMs appears 2.30% and 4.27% earlier, and the exothermic peak increases by 2.72% and 1.34%, respectively. The cumulative heat release of CCMs gradually decreases with an increasing content of MTs powder. When the replacement of MTs, FA, and SL is 15%, respectively, the second exothermic peak of CCMs increases by 1.34%, −16.13%, and −12.04% for MTs, FA, and SL, respectively. The final heat release of MTs is higher than that of FA, but lower than that of SL. The hydration process of CCMs undergoes three stages: nucleation and crystal growth (NG), interactions at phase boundaries (I), and diffusion (D).

Keywords: molybdenum tailings powder; mineral admixture; hydration heat; Krstulovic–Dabic model; hydration kinetics; kinetic parameters

check for updates

Citation: Cheng, Q.; Meng, W.; Ma, K. Hydration Heat and Hydration Kinetics of Cement Paste Compound with Molybdenum Tailings Powder: A Research Article. *Coatings* **2023**, *13*, 2073. https://doi.org/10.3390/coatings13122073

Academic Editor: Andrea Nobili

Received: 14 November 2023
Revised: 6 December 2023
Accepted: 8 December 2023
Published: 12 December 2023

1. Introduction

With the rapid economic development in China, there is also a growing demand for mineral resources. This has led to the extensive exploitation of various minerals, including molybdenum minerals. However, the ore grade of molybdenum deposits is low [1,2]. After separating the valuable metals from the ore, the majority (95% of the total) is discharged as molybdenum tailings [3,4]. The accumulation of molybdenum tailings not only occupies large amounts of land, but also pollutes the surrounding environment [5,6]. Therefore, the utilization of molybdenum tailings as a resource is of great significance in reducing environmental pollution and achieving a low-carbon economy. Using molybdenum tailings powder (MTs) as an admixture in cementitious materials can not only effectively reduce cement consumption and carbon emission, but also contribute to the sustainable development of resources and the environment [2–4,7].

Mineral admixtures are essential components of modern concrete. Studies have shown [8–14] that tailings containing SiO_2, Al_2O_3, CaO, and Fe_2O_3 can be used as concrete admixtures after being processed into fine powders. Han et al. [8] and Cheng et al. [9,10] confirmed the feasibility of using iron tailings powder as an admixture in concrete preparation. Geng [11] and Qiu et al. [14] reported that lead–zinc tailings powder can be used as an admixture in concrete preparation. Xu et al. [12] and Huang et al. [13] found that using copper tailings powder as a concrete admixture is feasible. Molybdenum tailings have

a chemical composition similar to that of iron, lead–zinc, and copper tailings. Therefore, MTs powder can be used as an admixture in concrete. However, different types of tailings, which are fine powders, exhibit varying performances as concrete admixtures due to differences in the beneficiation process and ore composition. It has also been shown [15–17] that the addition of copper, iron, or bauxite tailings powders reduces the rate of hydration and heat release in cement paste. Furthermore, there are variations in the hydration process of cement depending on the type of tailings powder used. Meanwhile, studies have shown [18–22] that molybdenum tailings can be used as a fine aggregate to replace natural sand or as an admixture to replace cement in preparing mortar or concrete. Geng et al. [23] conducted a study on the pozzolanic activity and hydration products of cementitious materials made from molybdenum tailings. They discovered that molybdenum tailings exhibited pozzolanic activity and resulted in the formation of ettringite and C-S-H gel. Gao et al. [24] showed that when the amount of superfine molybdenum tailings that is used in place of cement is less than 10%, it is beneficial for improving the freeze–thaw resistance and carbonation resistance of concrete. At present, research on the influence of molybdenum tailings as fine aggregate or admixture on the performance of mortar or concrete primarily focuses on macro-performance and micro-performance. Furthermore, the influence of MTs powder as an admixture on the early hydration process of composite cementitious materials (CCMs) is of great significance to the subsequent performance of CCMs. Therefore, further studying the influence of MTs on the hydration hardening mechanism and kinetics of CCMs is of great significance. It is important to investigate the properties of molybdenum tailings powder and cement cementitious materials and gain a comprehensive understanding of how MTs affect the early hydration process of cement. This will enhance the utilization rate of molybdenum tailings resources.

Presently, there are more methods available to investigate the hydration process and kinetics of CCMs [25–29], with the Krstulovic–Dabic model being the most commonly used. Krstulovic et al. [29] proposed a hydration kinetic model that can calculate the rate curve of the hydration reaction and the kinetic parameters. This model is based on hydration heat and can be used to determine the hydration process and kinetic parameters of the CCMs. Yan et al. [30,31] discovered that the Krstulovic–Dabic model can better characterize the hydration process of the CCMs when the fly ash (FA) content is not more than 65% and when the slag (SL) content does not exceed 70%. Cheng et al. [16] found that the Krstulovic–Dabic model can also simulate the hydration kinetics of cement–iron tailings powder composite cementitious materials. Therefore, the Krstulovic–Dabic model could be used to characterize the hydration process of CCMs with MTs.

In this paper, the MTs powder comes from Yichun Luming Mining Co., Ltd., Yichun, China. The hydration heat of the CCMs was measured using an isothermal calorimeter to investigate the influence of MTs on the hydration heat of cement. Based on the Krstulovic–Dabic model, the hydration process and kinetic parameters of the CCMs were calculated and analyzed. The influences of MTs, FA, and SL on the hydration heat and hydration kinetics of cement were compared and analyzed under the same dosage. Additionally, the influence of MTs on the early hydration process of cement was discussed. The purpose of this paper is to explore the influence of MTs powder as mineral admixture on the cement hydration process and to study whether it can promote the hydration process of cement. At the same time, compared with FA and SL, it is studied whether the performance of MTs is similar to FA and SL, and whether it is stronger than FA. This research aims to provide a theoretical and experimental basis for the efficient utilization of molybdenum tailings as a valuable resource.

Subtitle: The Influence of Molybdenum Tailings Powder on the Hydration Heat and Kinetics of Cement Paste and a Comparative Study of Molybdenum Tailings Powder with Fly Ash and Slag. (The experiment was conducted at Central South University in May 2023, China).

2. Hydration Kinetic Model

The hydration process of CCMs is generally divided into five stages: the initial interaction period (I), induction period (II), reaction acceleration period (III), deceleration period (IV), and slow interaction period (V) [32,33]. In early hydration, its heat release normally accounts for only about 5% of the total heat release, which can be ignored compared to the whole hydration process. Therefore, in the study of hydration kinetics, the influence of the first exothermic peak is generally ignored, and the simulation discussion begins at the end of the induction phase [34–36].

The Krstulovic–Dabic model shows the relationship between the hydration degree (α) and the hydration time (t), and the kinetic model is divided into the following three stages [29,37]:

Nucleation and crystal growth, NG

$$[-\ln(1-\alpha)]^{1/n} = K_1(t-t_0) = K_1'(t-t_0) \tag{1}$$

Interactions at phase boundaries, I

$$\left[1-(1-\alpha)^{1/3}\right]^1 = K_2 r^{-1}(t-t_0) = K_2'(t-t_0) \tag{2}$$

Diffusion, D

$$\left[1-(1-\alpha)^{1/3}\right]^2 = K_3 r^{-2}(t-t_0) = K_3'(t-t_0) \tag{3}$$

Differentiating Equations (1)–(3) yield Equations (4)–(6).

NG

$$d\alpha/dt = F_1(\alpha) = K_1' n(1-\alpha)[-\ln(1-\alpha)]^{(n-1)/n} \tag{4}$$

I

$$d\alpha/dt = F_2(\alpha) = K_2' \cdot 3(1-\alpha)^{2/3} \tag{5}$$

D

$$d\alpha/dt = F_3(\alpha) = K_3' \cdot 3(1-\alpha)^{2/3}/[2-2(1-\alpha)^{1/3}] \tag{6}$$

where α is the hydration degree; n is the reaction order; K_i and K_i' (i = 1, 2, 3) are the reaction rate constants of three hydration processes; t is the hydration time; t_0 is the end time of the induction period, which is the point at which the hydration exothermic rate starts to increase uniformly [38]; r is the reaction particle radius; and $d\alpha/dt$ is the hydration rate.

Based on the hydration heat test measured using isothermal calorimetry, the hydration heat release rate and accumulated heat release of CCMs were obtained. Formulas (7) and (8) were used to convert the hydration heat data into the data needed in the hydration kinetic model. The hydration kinetic formula (Equation (9)) proposed by Knudsen [39] was used to calculate the Q_{max}. The formula is as follows.

$$\alpha(t) = Q(t)/Q_{max} \tag{7}$$

$$d\alpha/dt = dQ/dt \cdot 1/Q_{max} \tag{8}$$

$$1/Q(t) = 1/Q_{max} + t_{50}/[Q_{max}(t-t_0)] \tag{9}$$

where $Q(t)$ is the heat released by time t; Q_{max} is the total heat release at the end of hydration; and t_{50} is the hydration time required for exothermic reaction to reach 50% of Q_{max}.

3. Experimental Procedure

3.1. Raw Materials

P.I 42.5 Portland cement (PC) satisfied Chinese GB 175 was supplied by China Fushun Aocell Technology Co., Ltd., Fushun, China. Molybdenum tailings powder (MTs) was obtained from Yichun Luming Mining Co., Ltd., China. The low-calcium class F fly ash (FA) and S95-grade fine slag (SL) were employed, produced by Xiangtan Power Plant and Xiangtan Steel Plant (Xiangtan, China), respectively. Distilled water was used. The photos of raw materials are shown in Figure 1, and their chemical compositions and physical properties are shown in Table 1. Table 2 lists the main technical indexes of MTs. The particle size distribution of raw materials is shown in Figure 2. The XRD pattern of MTs is shown in Figure 3a. The main mineralogical compositions of MTs are quartz, feldspar, mica and chlorite. The SEM pattern of MTs is shown in Figure 3b; the MTs particles have irregular shapes and rough surfaces.

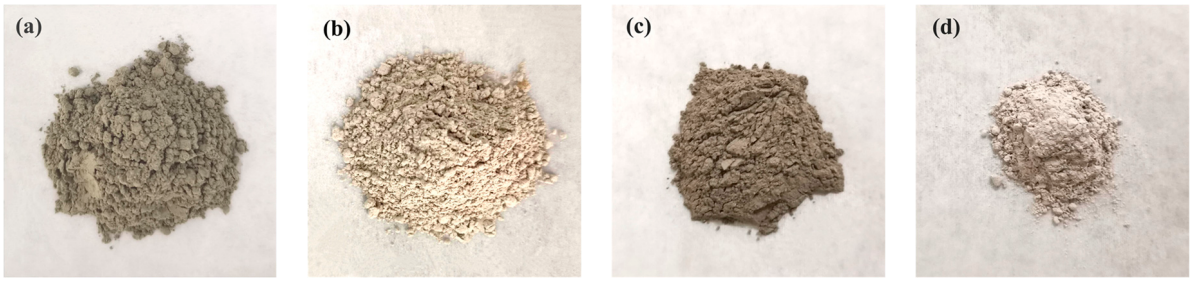

Figure 1. Raw materials. (**a**) PC, (**b**) MTs, (**c**) FA, (**d**) SL.

Table 1. Chemical compositions and physical properties of raw materials.

Materials	Chemical Composition (%)										LOI [1] (%)	SSA [2] (m^2/kg)	Density (g/cm^3)
	SiO_2	Al_2O_3	Fe_2O_3	CaO	MgO	SO_3	K_2O	Na_2O	MgO	MoO_3			
PC	20.84	4.68	3.56	63.43	3.29	2.30	—	0.55	—	—	1.48	358	3.11
MTs	67.75	13.84	2.71	2.75	1.14	2.24	5.45	1.77	1.14	0.0132	2.01	367	2.62
FA	52.70	25.80	9.70	3.70	1.20	0.20	1.16	0.79	0.88	—	4.20	434	2.35
SL	31.96	14.33	0.49	36.42	6.65	2.50	0.56	0.43	6.65	—	—	483	2.86

[1] Loss on ignition; [2] specific surface area.

Table 2. Main technical indexes of MTs.

Materials	Standard Consistency (%)	f-Cao	Setting Time (min)		Activity Index (%)		Water Demand Ratio (%)
			Initial	Final	7 d	28 d	
MTs	32.5	Eligible	386	540	75	69	109

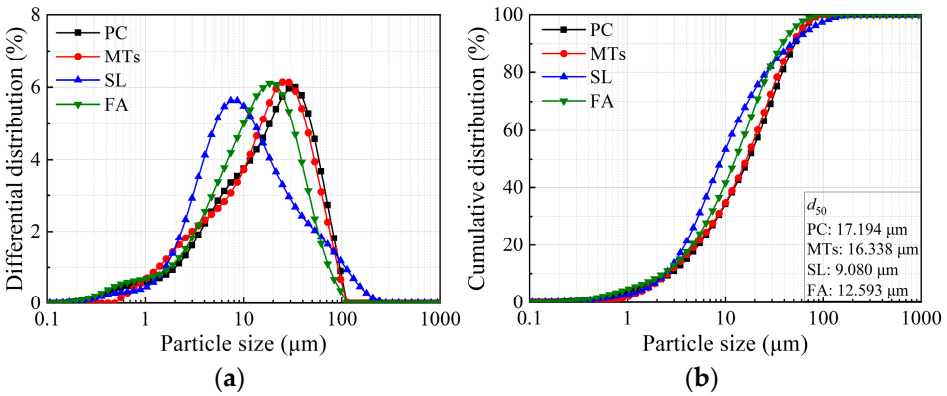

Figure 2. (**a**) Differential distribution and (**b**) cumulative distribution of raw materials.

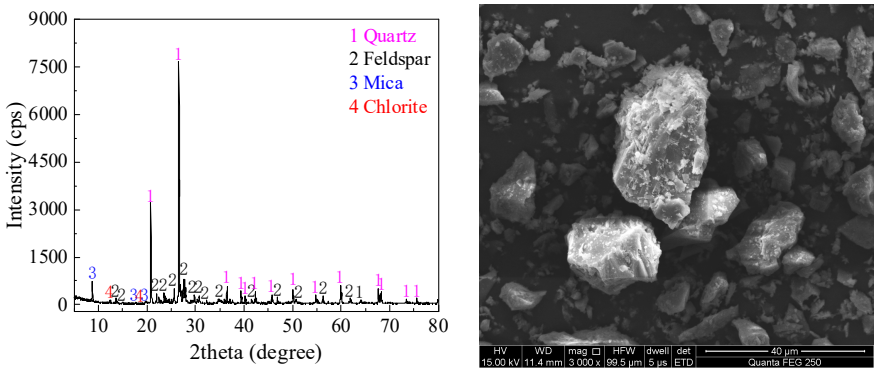

(**a**) (**b**)

Figure 3. (**a**) XRD pattern and (**b**) SEM pattern of MTs.

3.2. Mixture Proportions and Testing Methods

The mixture proportions of the CCMs pastes are summarized in Table 3. The MTs substitution rates were 0%, 5%, 15%, 25%, and 35%, the FA and SL replacement rates were both 15%, and the water-to-binder (w/b) ratio of 0.4 was used in this study.

Table 3. Mixture proportions.

Sample	Mass Fraction (%)					w/b
	PC	MTs	FA	SL	Water	
PC	100	0	—	—	40	0.4
MTs_5	95	5	—	—	40	0.4
MTs_{15}	85	15	—	—	40	0.4
MTs_{25}	75	25	—	—	40	0.4
MTs_{35}	65	35	—	—	40	0.4
FA_{15}	85	—	15	—	40	0.4
SL_{15}	85	—	—	15	40	0.4

An eight-channel TAM Air isothermal calorimeter was used to determine the exothermic characteristics of CCMs pastes. In the preparation of pastes, each CCMs sample was 50 g, and it had the same mixing periods (dry stirring for 60 s, slow and fast stirring for 60 s after adding water). The test temperature was set at 20 °C, and the test time was 120 h.

MTs were dried in an oven at 60 °C, the micro powder below 200 mesh was collected, and the sample was stored in a sealed bag. XRD was used to analyze the phase composition of the sample. The diffraction source was Cu target, the scanning range was 5–75, the step size was 0.02, and the scanning speed was 6°/min.

The micro-morphology of MTs was observed using an FEI Quanta FEG 250 environmental field scanning electron microscope.

4. Results

4.1. Effect of Hydration Heat

4.1.1. MTs Powder Content

The hydration heat of CCMs with different MTs powder contents is shown in Figure 4. As presented in Figure 4a, the end time of the induction period of CCMs is delayed, and the rate of heat release decreases with the increase in MTs. When the content of MTs is not more than 15%, the second exothermic peak of the CCMs is advanced, and its peak heat release is enhanced. When the content of MTs exceeds 15%, the second exothermic peak of CCMs is delayed, and its peak heat release decreases. The addition of MTs influences the peak pattern of the second exothermic peak of CCMs. The PC undergoes a relatively gentle exothermic phase before reaching the second peak of the exothermic reaction. However, as the MTs powder content increases, the gentle section before the peak of the second

exothermic peak of the CCMs gradually shortens until it disappears. Furthermore, the pozzolanic activity of MTs is activated in the later stage of hydration, and its pozzolanic effect leads to a higher heat release rate for MTs_5, MTs_{15}, MTs_{25}, and MTs_{35} compared to PC.

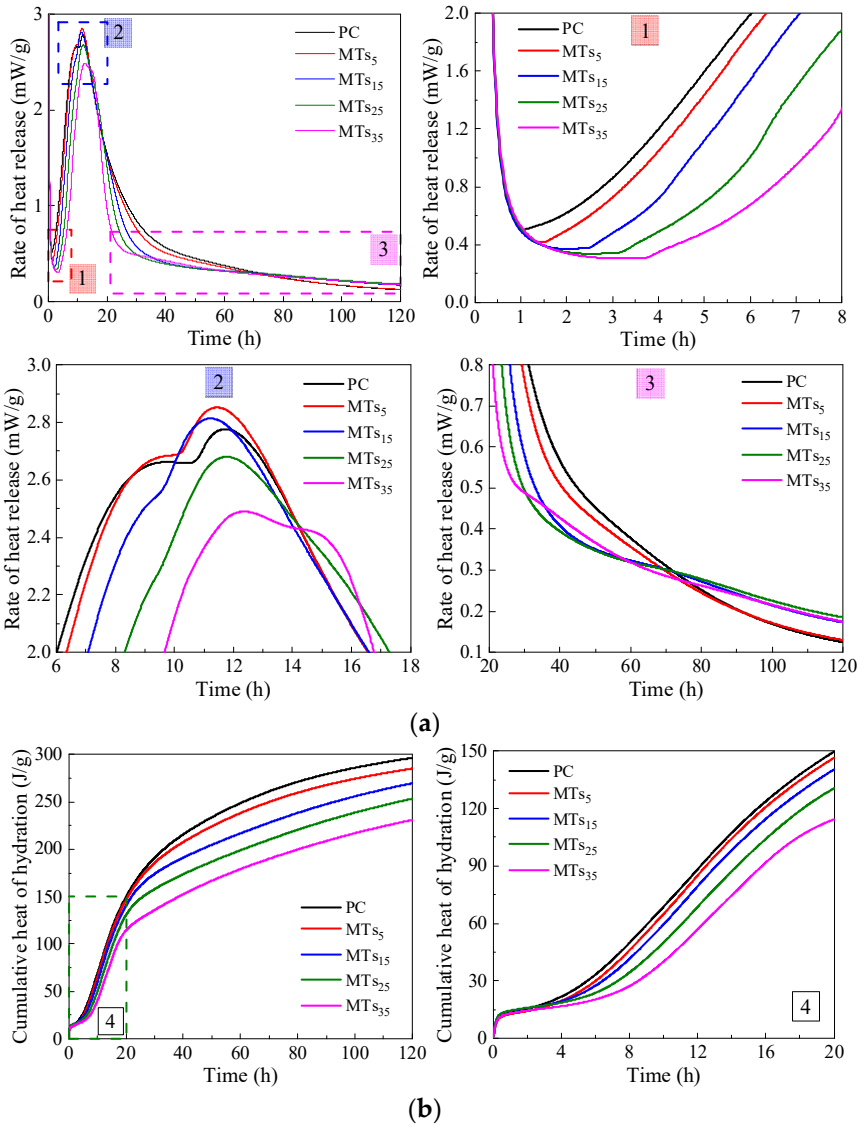

Figure 4. Influence of MTs powder content on hydration heat release of the CCMs (1~4 represent enlargements of corresponding parts). (**a**) Rate of heat release. (**b**) Cumulative heat of hydration.

As shown in Figure 4b, the cumulative heat release of CCMs gradually decreases with an increasing MTs powder content. When the hydration time is not more than 20 h, there are minimal differences in the cumulative heat release curves of MTs_5, MTs_{15}, and PC. However, the difference between the cumulative heat release curves of MTs_5 and MTs_{15} and that of PC gradually increases as the hydration time extends.

Table 4 presents the influence of the MTs powder content on the acceleration period of CCMs. The incorporation of MTs delays the end time (t_0) of the induction period of CCMs. Furthermore, as the amount of MTs increased, t_0 was progressively delayed. When the content of MTs increased from 0% to 35%, the time t_0 was delayed from 1.07 h to 3.72 h. Compared with PC, the times t_1 for MTs_5 and MTs_{15} to reach the second exothermic peak were 2.30% and 4.27% earlier, and the exothermic peak V was increased by 2.72% and 1.34%, respectively. MTs_{25} and MTs_{35} reached the second exothermic peak with a later time t_1 and a lower exothermic peak V. However, the incorporation of MTs shortened the time

from the end of the induction period to the second exothermic peak. This resulted in a shortened acceleration period ($t_1 - t_0$).

Table 4. Influence of MTs powder content on the acceleration period of CCMs.

Sample	t_0 (h)	t_1 (h)	($t_1 - t_0$) (h)	V (mW/g)
PC	1.07	11.72	10.65	2.7763
MTs_5	1.45	11.45	10.00	2.8518
MTs_{15}	2.50	11.22	8.72	2.8136
MTs_{25}	3.15	11.77	8.62	2.6801
MTs_{35}	3.72	12.31	8.59	2.4895

Note: t_0 is the end time of the induction period, t_1 is the time to reach the second exothermic peak, $t_1 - t_0$ is the acceleration period time, and V is the peak value of the second exothermic peak.

Table 5 indicates the relative percentage of hydration heat of CCMs. The relative percentage of hydration heat is the ratio of the hydration heat of CCMs with the mixture to the hydration heat of the reference sample [15]. It can be seen from Table 5 that the incorporation of MTs decreases the relative percentage of hydration heat in CCMs. With the extension of the hydration time, the relative percentage of hydration heat of CCMs gradually stabilizes, which is greater than the mass fraction of cement in CCMs. MTs powder has a certain potential for activity. However, in the early stage of hydration, the filler effect and nucleation of MTs play significant roles [40–43]. In the later stages of hydration, the pozzolanic activity of MTs is stimulated, resulting in a pozzolanic exothermic effect. As a result, the percentage of hydration heat is greater than the mass fraction of cement in CCMs.

Table 5. Relative percentage of hydration heat of CCMs (%).

Sample	3 h	6 h	12 h	24 h	48 h	72 h	96 h	120 h
PC	100	100	100	100	100	100	100	100
MTs_5	89	88	97	98	96	96	96	96
MTs_{15}	94	82	90	93	88	87	89	91
MTs_{25}	94	70	77	86	80	81	83	85
MTs_{35}	83	61	64	74	71	73	76	78

4.1.2. Mineral Admixture Types

Figure 5 shows the influences of MTs, FA, and SL with the same replacement ratio of 15% on the hydration heat of CCMs. According to Figure 5a, the incorporation of MTs, FA, and SL delays the end time of the induction period in the cementitious system, among which MTs powder has a significant influence on the end time of the induction period of CCMs, and the end time of the induction period of CCMs mixed with FA and SL is similar. The incorporation of MTs, FA, and SL reduces the heat release rate at the end of the induction period of CCMs, and the reduction range is similar, which decreases from 0.5 mW/g to about 0.35 mW/g. The incorporation of MTs, FA, and SL influences the peak value and peak pattern of the second exothermic peak of CCMs. The second exothermic peak of CCMs with MTs is advanced, and its peak heat release increases; the second exothermic peak of CCMs with FA is delayed, and its peak heat release decreases, and that of CCMs with SL is reduced. This shows that, compared with FA and SL, the same replacement ratio of MTs resulted in faster hydration products in CCMs during the acceleration period (as shown in Figure 5a-2). After 60 h of hydration of CCMs (as shown in Figure 5a-3), the hydration heat release rates of MTs_{15} and SL_{15} gradually exceed that of PC and FA_{15}.

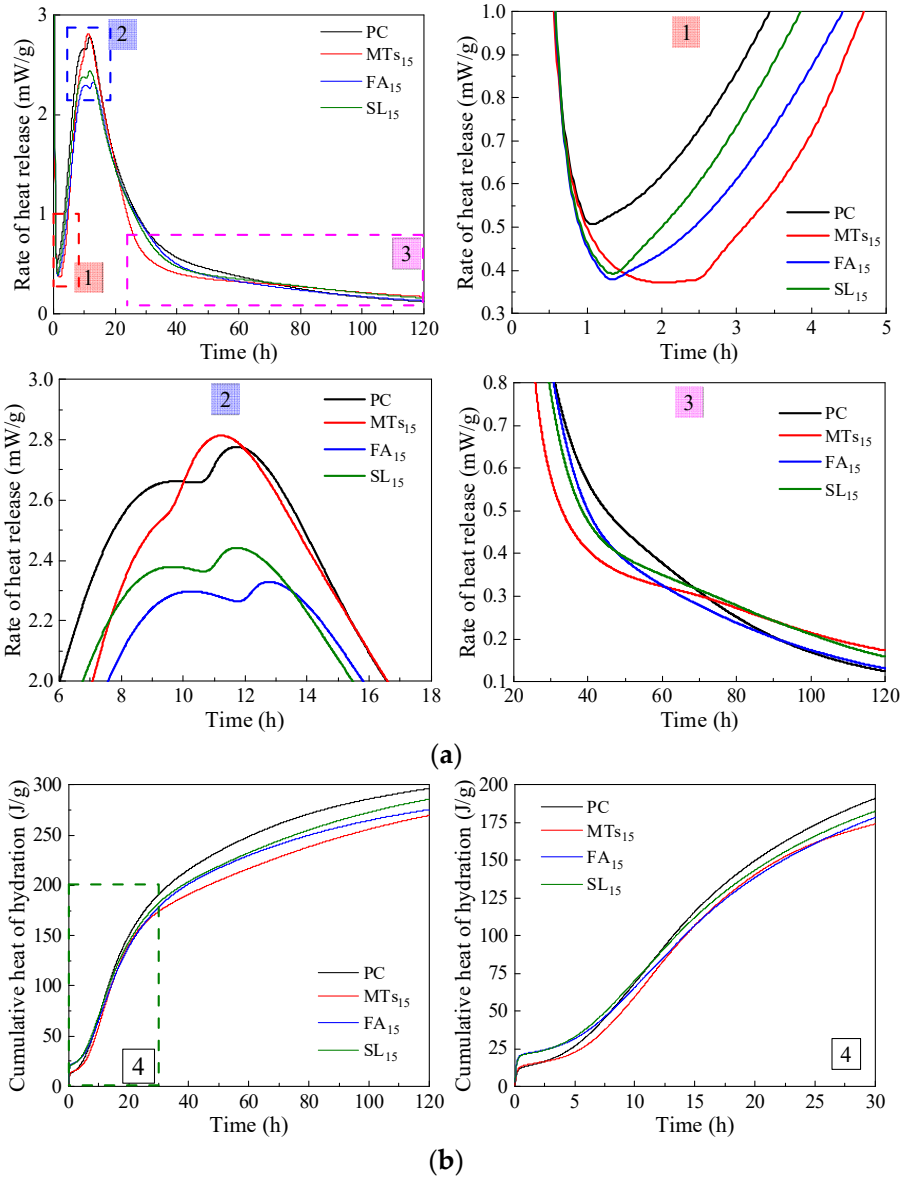

Figure 5. Influence of admixture types on hydration heat release of CCMs (1~4 is enlargements of corresponding parts). (**a**) Rate of heat release. (**b**) Cumulative heat of hydration.

According to Figure 5b, when the hydration time is not more than 30 h, the cumulative heat release curves of the PC, MTs_{15}, FA_{15}, and SL_{15} are similar. When the hydration time is 120 h, the order of cumulative heat release is PC > SL_{15} > FA_{15} > MTs_{15}.

The influences of different admixture types on the acceleration period of CCMs is presented in Table 6. The inclusion of MTs, FA, and SL prolongs the duration of the induction period in the cementitious system, with MTs having the most significant impact on its end time. The second exothermic peak of CCMs with MTs is advanced, and its peak heat release increases. On the other hand, the second exothermic peak of CCMs with FA or SL is delayed, and its peak heat release decreases. When the replacement of MTs, FA, and SL is 15%, respectively, the second exothermic peak of CCMs increases by 1.34%, −16.13%, and −12.04% for MTs, FA, and SL, respectively. The inclusion of FA extends the acceleration phase of CCMs, while the inclusion of MTs and SL reduces the acceleration phase of CCMs. The acceleration period of MTs_{15} is the shortest, indicating that the inclusion of MTs speeds up the hydration rate of CCMs and reduces the hydration time of CCMs.

Table 6. Influence of admixture types on the acceleration period of CCMs.

Sample	t_0 (h)	t_1 (h)	($t_1 - t_0$) (h)	V (mW/g)
PC	1.07	11.72	10.65	2.7763
MTs_{15}	2.50	11.22	8.72	2.8136
FA_{15}	1.33	12.77	11.44	2.3285
SL_{15}	1.33	11.73	10.40	2.4419

Table 7 shows the relative percentage of hydration heat for CCMs with MTs, FA, and SL, respectively. The relative percentages of hydration heat of MTs_{15} are 94% and 82% at 3 h and 6 h, respectively, which are lower than 100%. The relative percentages of hydration heat for FA_{15} are 139% at 3 h and 109% at 6 h. Similarly, the relative percentages of hydration heat for SL_{15} are 139% at 3 h and 115% at 6 h. These values are higher than 100%. With the increase in hydration time, the relative percentages of hydration heat for MTs_{15}, FA_{15}, and SL_{15} gradually approach 91%, 93%, and 96%, respectively. These values are all higher than the mass fraction of cement in CCMs. It shows that the pozzolanic activities of MTs, FA, and SL are activated during the stable hydration period. This results in a relative percentage of hydration heat that is greater than the mass fraction of cement in CCMs.

Table 7. Relative percentage of hydration heat for CCMs with MTs, FA, or SL (%).

Sample	3 h	6 h	12 h	24 h	48 h	72 h	96 h	120 h
PC	100	100	100	100	100	100	100	100
MTs_{15}	94	82	90	93	88	87	89	91
FA_{15}	139	109	93	93	93	92	92	93
SL_{15}	139	115	99	96	94	94	95	96

4.1.3. Total Heat Release

The hydration heat only measured the cumulative heat release of CCMs for 120 h. The total heat release Q_{max} of CCMs was derived based on the hydration heat data and the Knudsen formula (Equation (9)). In this study, PC was used as an example to determine the total heat release Q_{max} and the time t_{50} required to reach 50% of Q_{max}. The curve in Figure 6 was fitted linearly based on the hydration heat data. The calculation process of other groups was similar to that of the PC. The Knudsen formula, Q_{max}, and t_{50} are shown in Table 8. It can be seen from Table 8 that as the content of MTs powder increases, the Q_{max} of CCMs gradually decreases, and the time t_{50} gradually prolongs. This conclusion aligns with the findings of the hydration heat test.

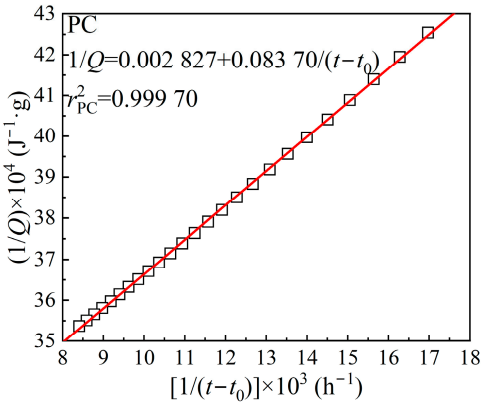

Figure 6. Determination of total heat release Q_{max} from linear regression.

Table 8. Knudsen formulas of CCMs.

Sample	Knudsen Formula	Q_{max} (J/g)	t_{50} (h)
PC	$1/Q = 0.002\,827 + 0.083\,70/(t - t_0)$	353.73	29.61
MTs_5	$1/Q = 0.002\,928 + 0.089\,04/(t - t_0)$	341.53	30.41
MTs_{15}	$1/Q = 0.002\,948 + 0.119\,85/(t - t_0)$	339.21	40.65
MTs_{25}	$1/Q = 0.003\,033 + 0.143\,69/(t - t_0)$	329.71	47.38
MTs_{35}	$1/Q = 0.003\,270 + 0.165\,03/(t - t_0)$	305.81	50.47
FA_{15}	$1/Q = 0.003\,094 + 0.102\,27/(t - t_0)$	323.21	33.05
SL_{15}	$1/Q = 0.002\,835 + 0.114\,00/(t - t_0)$	352.73	40.21

The Q_{max} can reflect the hydration trend and degree of CCMs to a certain extent. The higher the Q_{max} value, the greater the hydration degree of CCMs. According to Table 8, the Q_{max} of SL_{15} is the largest, followed by MTs_{15}. This is in contrast to the 120 h cumulative heat release obtained from the hydration heat test. The activation effect of MTs powder may be stronger than that of FA in the later stage, thus resulting in a gradual increase in its accumulated heat release, surpassing that of FA. Compared to FA_{15} and SL_{15}, the Q_{max} of MTs_{15} increased by 4.95% and decreased by 3.83%, respectively. This shows that the hydration degree of SL is higher, followed by MTs.

4.2. Hydration Kinetic Analysis

The Q_{max} of CCMs has been calculated according to the Knudsen formula. And the hydration degree (α) and hydration rate ($d\alpha/dt$) required by the Krstulovic–Dabic model can be obtained according to Formulas (7) and (8). Taking PC as an example, the kinetic parameters K_1' and n of stage NG can be derived by Formula (1) and by linearly fitting the curve of $\ln[-\ln(1-\alpha)]$ vs. $\ln(t - t_0)$, as shown in Figure 7a. The K_2' of stage I and K_3' of stage D can also be derived using Formulas (2) and (3) for linear fitting, respectively, as shown in Figure 7b,c. By substituting the parameters n, K_1', K_2', and K_3' into Formulas (4)–(6), the hydration reaction rate curves of NG, I, and D can be obtained. The hydration reaction rate curves and hydration kinetic parameters of other groups were similar to those of PC.

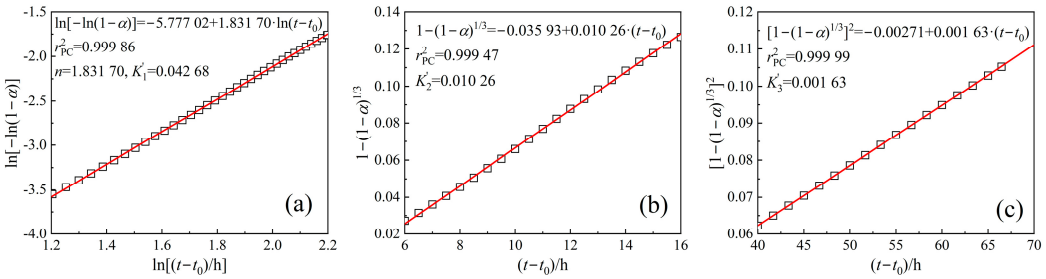

Figure 7. Determination of kinetic parameters n, K_1', K_2', and K_3' via linear regression. (**a**) n, K_1'; (**b**) K_2'; (**c**) K_3'.

4.2.1. Hydration Process Simulation of CCMs

Based on the Krstulovic–Dabic model, the hydration process is divided into three stages: nucleation and crystal growth, interactions at phase boundaries, and diffusion. These three stages may occur at the same time, but the whole process of the hydration depends on the slowest reaction stage [35,44]. In the early stages of hydration, the CCMs contain more water and fewer hydration products. As a result, the ion migration resistance is smaller, and the rate is faster. Consequently, the hydration process is controlled by NG. As the hydration time extends, the hydration products in the CCMs increase, and the structure becomes denser. Therefore, the resistance to ion migration is increased, resulting in a decrease in the migration rate. As a result, the hydration process is initially controlled by the I stage and then by the D stage [17].

The relationship between the hydration degree α and the hydration reaction rate $d\alpha/dt$ of CCMs is shown in Figure 8. The curves of $F_1(\alpha)$ and $F_2(\alpha)$ intersect with $F_3(\alpha)$ at α_1 and α_2, respectively. α_1 represents the transition point from the NG process to the I process, while α_2 represents the transition point from the I process to the D process. This shows that the incorporation of MTs, FA, and SL does not influence the hydration process of CCMs. The hydration process still undergoes three stages: NG-I-D. The Krstulovic–Dabic model can better simulate the hydration processes of NG, I, and D in CCMs, respectively.

According to Figure 8, when the MTs powder content is not more than 35%, the simulation effects of the NG, I, and late D stages of the hydration reaction with the hydration rate curve obtained from the hydration heat test are good. When the MTs powder content is 35%, the simulation effects of the NG and late D stages are better, while the simulation effect of the I stage deviates significantly from the reaction rate measured by the experiment. This is because the degree of influence of MTs on the total hydration reaction of CCMs increases with the MTs powder content, and the deviation of the simulation gradually increases with the MTs powder content. When the contents of MTs, FA, and SL are all 15%, the Krstulovic–Dabic model has a better simulation effect on FA, SL, and MTs. However, the simulation effect of the pre-D stage deviates from the actual data due to the weak pozzolanic effect caused by the admixture during late hydration.

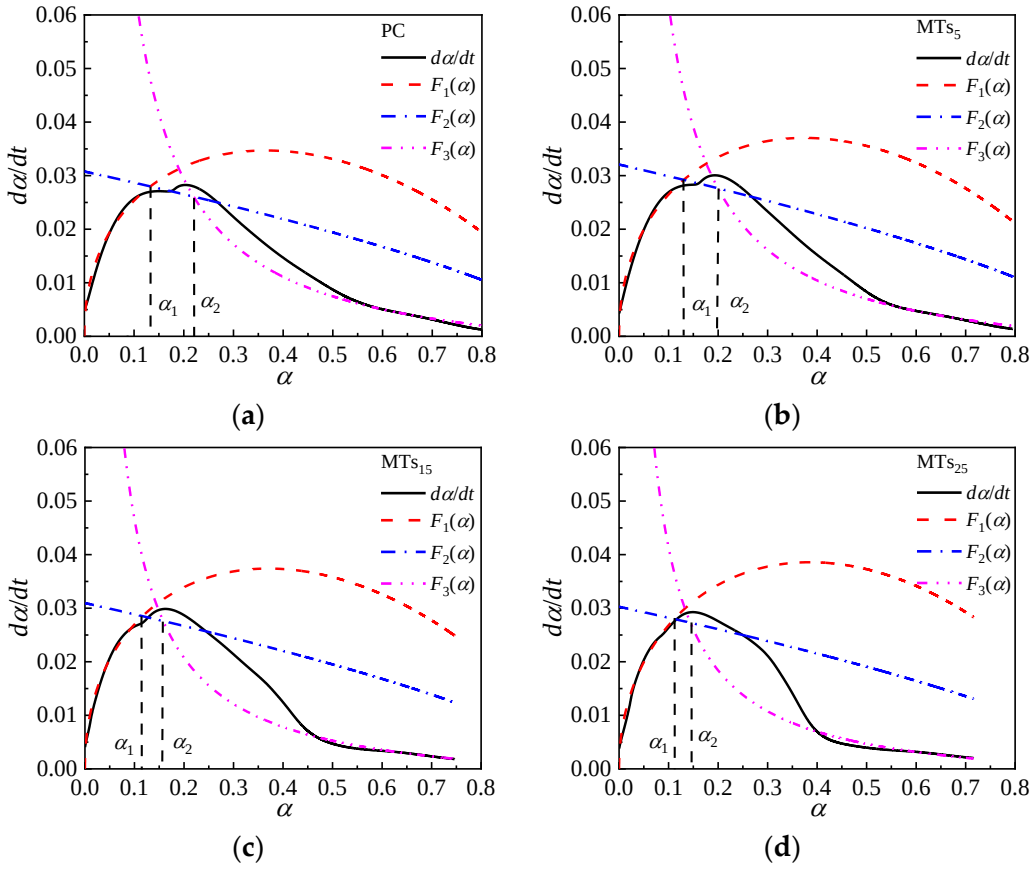

Figure 8. *Cont.*

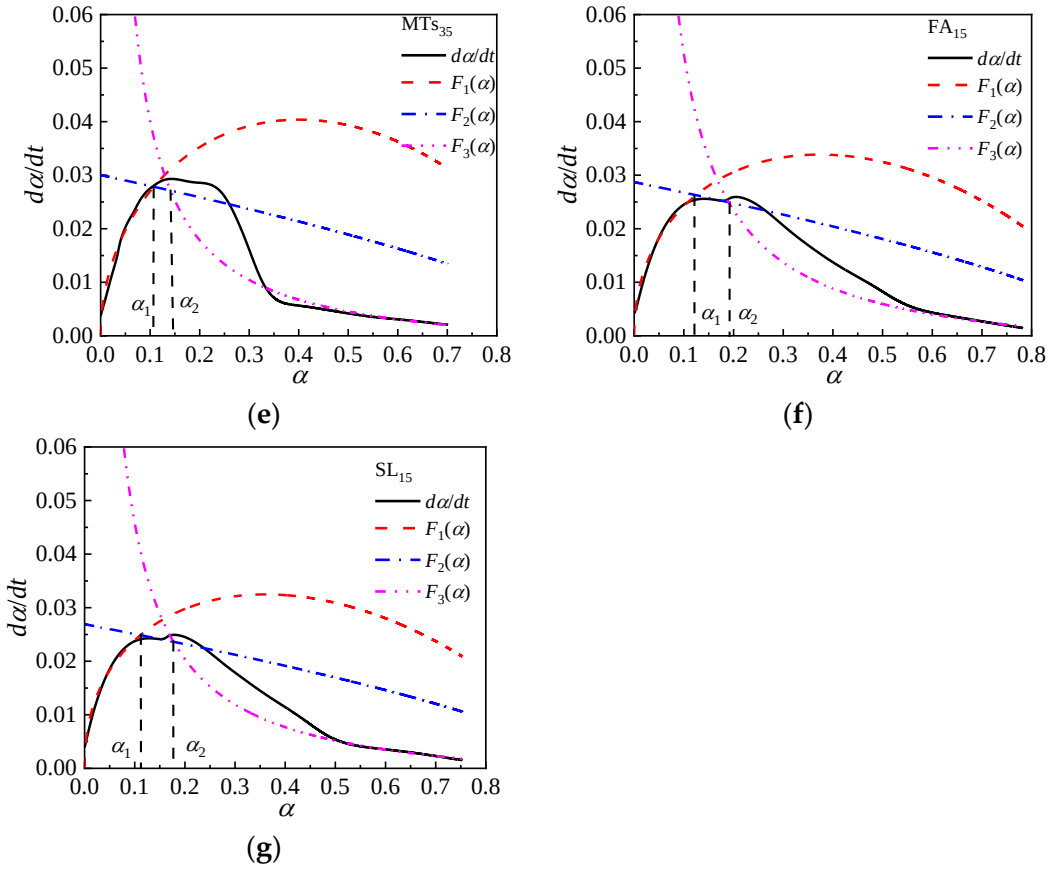

Figure 8. Hydration rate curves for CCMs. (**a**) PC; (**b**) MTs_5; (**c**) MTs_{15}; (**d**) MTs_{25}; (**e**) MTs_{35}; (**f**) FA_{15}; (**g**) SL_{15}.

4.2.2. Hydration Kinetic Parameters of CCMs

The hydration kinetic parameters of CCMs are presented in Table 9. The reaction order n, the nucleation of crystallization, and the production of hydration products of the CCMs were calculated in [45]. The higher the value of n, the greater the reaction resistance of CCMs [16,46]. The n of the CCMs gradually increases with the increasing MTs powder content. This shows that the introduction of MTs has reached the reaction resistance in the crystallization process of hydration products in CCMs, and the most significant influence is observed with an MTs powder content of 35% [29,31]. When the contents of MTs, FA and SL are all 15%, the order of n of the CCMs is FA_{15} > MTs_{15} > SL_{15}. This indicates that MTs, FA, and SL have different influences on the nucleation effect. Furthermore, the influence of FA on the crystallization process of the hydration products of CCMs is greater than that of MTs and SL.

Table 9. Hydration kinetic parameters of CCMs.

Sample	n	K_1'	K_2'	K_3'	α_1	α_2	$\alpha_2 - \alpha_1$
PC	1.831 70	0.042 68	0.010 26	0.001 63	0.133	0.220	0.087
MTs_5	1.881 52	0.044 87	0.010 69	0.001 53	0.130	0.199	0.069
MTs_{15}	1.860 04	0.045 61	0.010 32	0.001 15	0.116	0.158	0.042
MTs_{25}	1.949 23	0.045 73	0.010 09	0.001 02	0.111	0.144	0.033
MTs_{35}	2.047 24	0.046 34	0.010 01	0.000 99	0.107	0.141	0.034
FA_{15}	1.878 14	0.041 04	0.009 57	0.001 30	0.124	0.190	0.066
SL_{15}	1.810 73	0.040 21	0.008 97	0.001 13	0.111	0.177	0.066

The reaction rate constant K_1' of the NG process gradually increases with an increasing content of MTs. The incorporation of MTs increases the effective water-to-cement (w/c)

ratio of CCMs. Additionally, MTs can serve as nucleation sites to enhance the rate of hydration reaction. The reaction rate constant K_2' of the I process initially increases and then decreases with the increase in MTs powder content. When the content of MTs is small, the addition of MTs disperses the non-hydrated cement particles in the paste. This leads to an increase in the contact area between cement and water, resulting in an increase in the degree of hydration and improving the reaction rate. When the MTs powder content is high, the cement content decreases, and the concentration of Ca^{2+} in CCMs decreases. This delay in the time for $Ca(OH)_2$ crystals to reach saturation results in a decrease in the hydration reaction rate. The reaction rate constant K_3' of the D process gradually decreases with an increase in the MTs powder content. This is because the hydration products in the paste increase during the later stages of hydration. Furthermore, the filling effect of MTs fills the pores, while the pozzolanic effect of MTs promotes the generation of hydration products. This leads to a denser structure, which, in turn, increases the resistance to ion migration and reduces the rate of hydration reaction. When the contents of MTs, FA, and SL are all 15%, the K_1' and K_2' parameters of MTs_{15} are greater than those of FA_{15} and SL_{15}. This indicates that the reaction rate of crystallization nucleation and the phase boundary reaction of hydration products of paste with MTs are higher than those of FA and SL. Additionally, the hydration heat release rate of the CCMs in the acceleration period is larger. The K_3' value of MTs_{15} is smaller than that of FA and larger than that of SL, indicating that the reaction rate of MTs in the diffusion process is lower than that of FA but higher than that of SL.

The hydration degree α_1 gradually decreases with the increasing content of MTs, indicating that MTs shorten the NG process of CCMs. Furthermore, the higher the amount of MTs, the more pronounced the shortening becomes. This is because the incorporation of MTs accelerates the hydration rate, shortens the time for crystal nucleation and growth, and ultimately shortens the NG process. The $\alpha_2 - \alpha_1$ ratio gradually decreases as the content of MTs increases, indicating that MTs shorten the I process of CCMs. When the contents of MTs, FA, and SL are all 15%, the α_1 of MTs_{15} is lower than that of FA_{15} and higher than that of SL_{15}. The difference in α_1 indicates that mineral admixtures have varying influences on the NG process, with the greatest influence being from SL. The α_2 and $\alpha_2 - \alpha_1$ parameters of MTs_{15} are smaller than those of FA_{15} and SL_{15}, indicating that the incorporation of admixtures shortens the I process. Additionally, the influence of MTs on the I process is the greatest.

5. Discussion

The incorporation of MTs powder influences the heat release rate and cumulative heat release of CCMs due to its crystallization nucleation and pozzolanic effect. The crystallization nucleation and pozzolanic effect of MTs occur in the hydration acceleration period and the hydration stable period of CCMs, respectively [30,31,43,47,48]. Meanwhile, the incorporation of MTs reduces the proportion of cement clinker in CCMs and influences the effective w/c ratio of CCMs. Therefore, when the content of MTs is small, the effective w/c ratio of CCMs increases. Moreover, cement particles wrap around MTs particles, and the surfaces of MTs particles act as crystallization nucleation sites. This provides more nucleation points, increases the formation rate of hydration products such as C-S-H gel, and enhances the rate of hydration heat release. However, when the MTs content is higher, the proportion of cement clinker in CCMs significantly decreases, and the promotion effect of the crystallization nucleation of MTs is not significant. Therefore, the hydration heat release rate is reduced. Furthermore, in the later stage of hydration, the formation of $Ca(OH)_2$ increases the pH value, which stimulates the pozzolanic activity of MTs. This promotes the secondary hydration reaction of CCMs, resulting in the generation of hydration products such as C-S-H gel and a slight increase in the rate of hydration heat release.

The incorporation of MTs reduces the proportion of cement clinker and the concentration of Ca^{2+} in CCMs, therefore prolonging the nucleation time of $Ca(OH)_2$ and delaying the end time of the induction period [30]. When the MTs powder content is small, the

dilution effect of MTs and the surface of MTs act as crystallization nucleation sites in CCMs, thus promoting the hydration of CCMs and increasing their hydration heat release rate. When the MTs powder content is larger, the proportion of cement clinker in CCMs is significantly reduced, and MTs powder has a lower promoting effect on cement hydration, which reduces the hydration heat release rate of CCMs.

MTs, FA, and SL play similar roles in CCMs. In the hydration acceleration period, they are mainly involved in crystallization nucleation. In the hydration stable period, the pozzolanic effect mainly occurs to promote the secondary hydration of CCMs. Studies have shown [43,49] that the specific surface area and surface properties of the admixture will influence its nucleation role, and the nucleation role of the SL in the hydration acceleration period is stronger than that of FA. It can be seen from Table 1 that the specific surface areas and surface properties of MTs, FA, and SL are different, so their effects on the hydration heat release of cement are also different. In the meantime, the differences of MTs, FA, and SL of the potential activity resulted in different activities excited in the later stage of hydration. Therefore, the hydration heat release rate and cumulative heat release of CCMs are different with different intensities of the pozzolanic effect. This leads to different effects of MTs, FA, and SL on the hydration process.

6. Conclusions and Prospects

(1) The incorporation of MTs powder prolongs the end time of the induction period (t_0 increases) and shortens the acceleration period of CCMs (t_1–t_0 shortens). When the content of MTs is not more than 15%, the second exothermic peak of CCMs appears earlier and the peak heat release value increases. When the content of MTs exceeds 15%, the second exothermic peak of CCMs appears later, and the peak heat release value decreases. The cumulative heat release of CCMs gradually decreases with an increasing MTs powder content, but the relative percentage of hydration heat is greater than the mass fraction of cement in the paste.

(2) When the contents of MTs, FA, and SL are all 15%, compared with FA and SL, the influence of MTs powder on the extension of the end time of the induction period of CCMs is the most significant, the second exothermic peak of CCMs with MTs is advanced, and its peak heat release increases. When the hydration time is 120 h, the cumulative heat release of FA and SL is greater than that of MTs. Based on the final cumulative heat release calculated by the Knudsen formula, the Q_{max} of MTs exceeds that of FA. Compared with FA_{15} and SL_{15}, the Q_{max} of MTs_{15} is increased by 4.95% and −3.83%, respectively.

(3) The hydration process of CCMs undergoes three stages: nucleation and crystal growth (NG), interactions at phase boundaries (I), and diffusion (D). The relationship curve between the hydration degree and hydration reaction rate, calculated based on the Krstulovic–Dabic model, can better simulate the hydration reaction rate curve measured by the hydration heat test. With the increase in the MTs powder content, the reaction order n and K_1' of CCMs increase, K_2' increases first and then decreases, and K_3', α_1, and α_2 decrease. The incorporation of MTs shortens the NG and I process of CCMs.

The research in this paper shows that MTs powder as an admixture can enhance the hydration process of cement. Its performance is slightly superior to that of FA, which can help alleviate the shortage of FA. The use of MTs powder in new construction materials is not only beneficial for recycling waste resources but also for preserving the local environment. However, theoretical research on new building materials using MTs powder as the primary raw material is not sufficiently in-depth, and the controllability is not stable enough. Meanwhile, most of the research is still in the experimental stage, and industrial production has not been achieved.

Author Contributions: Data curation, formal analysis, writing—original draft preparation, and writing—review and editing, Q.C.; resources, supervision, and writing—review and editing, W.M.; investigation, methodology, and conceptualization, K.M. All authors have read and agreed to the published version of the manuscript.

Funding: This research was funded by Graduate School-enterprise Joint Innovation Project of Central South University (no. 1053320220028) and China Railway Resources Science and Technology Program Project (no. LM (2022)-F-53).

Institutional Review Board Statement: Not applicable.

Informed Consent Statement: Not applicable.

Data Availability Statement: The data presented in this study are available upon request from the corresponding author.

Conflicts of Interest: The authors declare no conflict of interest.

References

1. Yu, L. Overview of the latest research progress on comprehensive utilization of molybdenum tailings resources. *Metall. Mater.* **2021**, *41*, 21–22. (In Chinese)
2. Hu, B.L.; Wang, K.S.; Hu, P.; Yang, F.; Yu, Z.; Tan, J.; Song, R.; Zhao, B.; Cao, W. Research Progress of Molybdenum Tailings Resources Recycling and Utilization. *Mater. Rev.* **2015**, *29*, 123–127. (In Chinese)
3. Wu, H.Q.; Liu, C.; Chen, Y.F. Research Progress of and Comprehensive Utilized on Molybdenum Tailings Resources in China. *Met. Mine* **2018**, *8*, 169–174. (In Chinese)
4. Li, F.; Cui, X.W.; Liu, X.; Liu, Y.; Liu, M.; Zhang, G.; Zhou, C.; Fan, X. Research Progress in Secondary Utilization of Molybdenum Tailings in Building Materials. *Multipurp. Util. Miner. Resour.* **2021**, *3*, 132–139. (In Chinese)
5. Luo, T.; Yi, Y.; Sun, Q.; Li, L.G.; Tang, L.; Hua, C. The effects of adding molybdenum tailings as cementitious paste replacement on the fluidity, me-chanical properties and micro-structure of concrete. *J. Build. Eng.* **2022**, *62*, 105377. [CrossRef]
6. Quan, X.; Wang, S.; Li, J.; Luo, J.; Liu, K.; Xu, J.; Zhao, N.; Liu, Y. Utilization of molybdenum tailings as fine aggregate in recycled aggregate concrete. *J. Clean. Prod.* **2022**, *372*, 133649. [CrossRef]
7. Hu, G.S.; Zhang, C.; Qian, C.Y.; Wen, J.X. Recent Research Progress of Comprehensive Utilization of Molybdenum Tailings Re-sources. *Mater. Rev.* **2019**, *33*, 233–238. (In Chinese)
8. Han, F.; Luo, A.; Liu, J.; Zhang, Z. Properties of high-volume iron tailing powder concrete under different curing conditions. *Constr. Build. Mater.* **2020**, *241*, 118108. [CrossRef]
9. Cheng, Y.H.; Huang, F.; Qi, S.S.; Li, W.C. Effects of High-Silicon Iron Tailings on Carbonation and Sulphate Corrosion Resistance of Concrete. *J. Northeast. Univ. (Nat. Sci.)* **2019**, *40*, 121–125, 149. (In Chinese)
10. Cheng, Y.; Huang, F.; Li, W.; Liu, R.; Li, G.; Wei, J. Test research on the effects of mechanochemically activated iron tailings on the com-pressive strength of concrete. *Constr. Build. Mater.* **2016**, *118*, 164–170. [CrossRef]
11. Geng, B.Y. Preparation of High Performance Concrete Mixture with Lead-Zinc Ore Tailings from Youxi, Fujian Province. Ph.D. Thesis, University of Science and Technology Beijing, Beijing, China, 2016. (In Chinese)
12. Xu, W.; Lu, Y.; Shi, Q.; Yan, J.; Jie, X.; Zhou, X.; Liu, S. Research on application of copper tailings admixture in ready-mixed concrete. *New Build. Mater.* **2021**, *48*, 12–15. (In Chinese)
13. Huang, X.Y.; Ni, W.; Wang, Z.J.; Qian, J.W.; Zhu, L.P. Experimental study on autoclaved aerated concrete made from copper tailings without using lime as calcareous materials. *Mater. Sci. Technol.* **2012**, *20*, 11–15. (In Chinese)
14. Qiu, X.J.; Ni, W. Preparation of High Strength Concrete Using Fujian Lead-zinc Tailings and Slag Powder. *Met. Mine* **2015**, 176–180. (In Chinese)
15. Zhu, J.L.; Song, J.W.; Wang, L.; Xiao, L.N.; Liu, F.H. Hydration Heat and Kinetics of Copper Slag Powder-Cement Composite Cementitious System. *J. Build. Mater.* **2020**, *23*, 1282–1288. (In Chinese)
16. Cheng, Y.H.; Sun, X.H.; Zhang, J.Y. Hydration kinetics of cement–iron tailing powder composite cementitious materials and pore structure of hardened paste. *Constr. Build. Mater.* **2023**, *370*, 130673.
17. Zhou, L.F.; Gou, M.F.; Guan, X.M. Hydration kinetics of cement-calcined activated bauxite tailings composite binder. *Constr. Build. Mater.* **2021**, *301*, 124296. [CrossRef]
18. Gao, S.; Cui, X.; Kang, S.; Ding, Y. Sustainable applications for utilizing molybdenum tailings in concrete. *J. Clean. Prod.* **2020**, *266*, 122020. [CrossRef]
19. Sun, M.; Fu, Y.; Wang, W.; Yang, Y.; Wang, A. Experimental Research on the Compression Property of Geopolymer Concrete with Molyb-denum Tailings as a Building Material. *Buildings* **2022**, *12*, 1596. [CrossRef]

20. Luo, T.; Yi, Y.; Liu, F.; Sun, Q.; Pan, X.; Hua, C. Early-age hydration and strength formation mechanism of composite concrete using molybdenum tailings. *Case Stud. Constr. Mater.* **2022**, *16*, e1101. [CrossRef]
21. Quan, X.; Wang, S.; Liu, K.; Xu, J.; Zhao, N.; Liu, B. Evaluation of molybdenum tailings as replacement for fine aggregate in concrete: Me-chanical, corrosion resistance, and pore microstructural characteristics. *Constr. Build. Mater.* **2022**, *343*, 127982. [CrossRef]
22. Quan, X.; Wang, S.; Liu, K.; Xu, J.; Zhao, N.; Liu, B. Influence of molybdenum tailings by-products as fine aggregates on mechanical prop-erties and microstructure of concrete. *J. Build. Eng.* **2022**, *54*, 104677. [CrossRef]
23. Geng, B.; Wang, Z.; Shi, S.; Wang, K.; Fu, J.; Wen, Z.; Guo, X. Pozzolanic Reactivity and Hydration Products of Cementitious Material Prepared Using Mo-lybdenum Tailings. *Processes* **2023**, *11*, 1101. [CrossRef]
24. Gao, S.; Cui, X.; Zhang, S. Utilization of Molybdenum Tailings in Concrete Manufacturing: A Review. *Appl. Sci.* **2020**, *10*, 138. [CrossRef]
25. Wang, P.M.; Feng, S.X.; Liu, X.P. Research Approaches of Cement Hydration Degree and Their Development. *J. Build. Mater.* **2005**, *8*, 646–652. (In Chinese)
26. Wu, X.Q. Study on hydration kinetics of slag cement. *J. Chin. Ceram. Soc.* **1988**, 423–429. (In Chinese)
27. Merzouki, T.; Bouasker, M.; Khalifa, N.E.H.; Mounanga, P. Contribution to the modeling of hydration and chemical shrinkage of slag-blended cement at early age. *Constr. Build. Mater.* **2013**, *44*, 368–380. [CrossRef]
28. Kolani, B.; Buffo-Lacarrière, L.; Sellier, A.; Escadeillas, G.; Boutillon, L.; Linger, L. Hydration of slag-blended cements. *Cem. Concr. Compos.* **2012**, *34*, 1009–1018. [CrossRef]
29. Krstulović, R.; Dabić, P. A conceptual model of the cement hydration process. *Cem. Concr. Res.* **2000**, *30*, 693–698. [CrossRef]
30. Han, F.H. Study on Hydration Characteristics and Kinetics of Composite Binder. Ph.D. Thesis, China University of Mining & Technology, Beijing, China, 2015. (In Chinese)
31. Han, F.H.; Wang, D.M.; Yan, P.Y. Hydration Kinetics of Composite Binder Containing Different Content of Slag or Fly Ash. *J. Chin. Ceram. Soc.* **2014**, *42*, 613–620. (In Chinese)
32. Yin, B.; Kang, T.; Kang, J.; Chen, Y.; Wu, L.; Du, M. Investigation of the hydration kinetics and microstructure formation mechanism of fresh fly ash cemented filling materials based on hydration heat and volume resistivity characteristics. *Appl. Clay Sci.* **2018**, *166*, 146–158. [CrossRef]
33. Adamtsevich, A.; Pustovgar, A. Effect of Modifying Admixtures on the Cement System Hydration Kinetics. *Appl. Mech. Mater.* **2015**, *725–726*, 487–492. [CrossRef]
34. Chen, X.; Yang, H.; Shi, Y.; Zhang, J. Hydration Characteristics of Cement-Based Materials with Incorporation of Phosphorus Slag Powder. *J. Build. Mater.* **2016**, *19*, 619–624. (In Chinese)
35. Yan, P.Y.; Zheng, F. Kinetics Model for the Hydration Mechanism of Cementitious Materials. *J. Chin. Ceram. Soc.* **2006**, *34*, 555–559. (In Chinese)
36. Wang, T.; Xue, Y.; Zhou, M.; Lv, Y.; Chen, Y.; Wu, S.; Hou, H. Hydration kinetics, freeze-thaw resistance, leaching behavior of blended cement containing co-combustion ash of sewage sludge and rice husk. *Constr. Build. Mater.* **2017**, *131*, 361–370. [CrossRef]
37. Liu, S.H.; Li, Q.L.; Zhao, X.Y. Hydration Kinetics of Composite Cementitious Materials Containing Copper Tailing Powder and Graphene Oxide. *Materials* **2018**, *11*, 2499. [CrossRef]
38. Liu, Z.H. Study on the Mechanism of Hydration Induction Period of Portland Cement. Master's Thesis, Guangzhou University, Guangzhou, Chian, 2023. (In Chinese)
39. Knudsen, T. The dispersion model for hydration of portland cement I. *Gen. Concepts. Cem. Concr. Res.* **1984**, *14*, 622–630. [CrossRef]
40. Wang, C.L.; Ye, P.F.; Zhang, K.F.; Han, G.S.; Huo, Y.K.; Zhao, G.F.; Ren, Z.Z. Study on Preparation and Hydration Mechanism of Composite Cementitious Materials using Molybdenum Tailings. *Met. Mine* **2020**, 41–47. (In Chinese)
41. Zhang, Y.J.; Fu, S.F.; Zhang, G.T.; Yan, L.C. Study on the Influence of Molybdenum Tailings Powder on the Strength and Micro-structure of Cement-based Materials. *Met. Mine* **2023**, 253–259. (In Chinese)
42. Quan, Z.Z.; Feng, X.L.; Chen, Y.Y. Study on the preparation of reactive powder concrete with molybdenum tailings. *New Build. Mater.* **2022**, *49*, 46–49. (In Chinese)
43. Yan, P.Y.; Zhang, Z.Q. Review on Hydration of Composite Cementitious Materials. *J. Chin. Ceram. Soc.* **2017**, *45*, 1066–1072. (In Chinese)
44. Lyu, X.; Yao, G.; Wang, Z.; Wang, Q.; Li, L. Hydration kinetics and properties of cement blended with mechanically activated gold mine tailings. *Thermochim. Acta* **2020**, *683*, 178457. [CrossRef]
45. Bezjak, A. Nuclei growth model in kinetic analysis of cement hydration. *Cem. Concr. Res.* **1986**, *16*, 605–609. [CrossRef]
46. Zhou, L.; Gou, M.; Luo, S. Hydration kinetics of a calcination activated bauxite tailings-lime-gypsum ternary system. *J. Build. Eng.* **2021**, *38*, 102189. [CrossRef]
47. Deng, S.; Liu, L.; Yang, P.; Zhang, C.; Lv, Y.; Xie, L. Experimental Study on Early Strength and Hydration Heat of Spodumene Tailings Cemented Backfill Materials. *Materials* **2022**, *15*, 8846. [CrossRef]

48. Chen, J.; Shui, Z.H.; Sun, T.; Gao, X.; Song, Q.; Guo, C. Early Hydration Kinetics Research of Calcined Coal Gangue in Cement-Based Materials. *Bull. Chin. Ceram. Soc.* **2019**, *38*, 1983–1990. (In Chinese)
49. He, J.; Long, G.; Ma, K.; Xie, Y. Influence of fly ash or slag on nucleation and growth of early hydration of cement. *Thermochim. Acta* **2021**, *701*, 178964. [CrossRef]